Response Analysis of Thoracic Cage against Blunt Loading using Human FE Model

Yuichi Ito , Yasuki Motozawa , Fumie Mori

Abstract The objective of this study is to develop maps representing local stiffness and tolerance of the occupant's thorax using finite element (FE) models. To reduce thoracic injuries to occupants, it would be beneficial to identify load paths from restraint systems to the thorax that provide higher stiffness in order to absorb higher kinetic energy of the occupant during a frontal collision. In this study, local thoracic response analysis against blunt loading was conducted by using age-specific human occupant FE models and rigid impactor models. In addition, the effect of aging on the local response of the rib cage was investigated. Local stiffness of the thoracic cage was calculated by assuming a linear stiffness curve and using the energy absorbed up to 50 mm chest deflections. Local tolerance of the thoracic cage was defined from the value of the deflection where the element elimination was initially activated on the rib. The distribution maps established through the present research quantitatively identified the difference of stiffness and tolerance between 35 years old and 75 years old. They will also enable the assessment of the restraint system relative to the occupant's thorax.

Keywords finite element method, human, elderly, occupant, thoracic response

I. INTRODUCTION

The percentage of the elderly population has been rapidly increasing in most developed countries in recent years. For example, the 65 years and older (hereafter 65+ Y/O) age group is 23.1% of the population in 2011 according to the Statistics Bureau of Japan [1]. The 65+ Y/O age group numbered 40.4 million in 2010, an increase of 5.4 million or 15.3% since 2000 in the US [2]. In Japan, the proportion of the 65+ Y/O age group in traffic accident fatalities has been increasing, while the number of traffic fatalities has been decreasing steadily in the last couple of decades [3]. In 2011, occupant and pedestrian fatalities accounted for 39% and 47%, respectively, of all traffic fatalities in people 65+ Y/O in Japan [3]. Therefore, protection of the elderly has become an important societal issue. According to Japanese traffic statistics research [4-5], the older occupant of 65+ Y/O was more likely to sustain injury to the thorax compared with the under 65 Y/O in the case of frontal traffic accidents. Ridella et al. [6] analyzed data from the National Automotive Sampling System ‐ Crashworthiness Data System (NASS ‐ CDS) and the Crash Injury Research Engineering Network (CIREN) cases and found that the crash severity was consistently lower for the older age groups and outcomes were worse in the older occupants even for similar crash severity and injury. Since the stiffness and tolerance of the human body changes with age, elderly occupants may possibly sustain thoracic injury during low-energy impact even if they are belted due to the fragility of the thoracic cage. To reduce thoracic injuries to occupants in frontal collisions, we have been endeavoring to minimize the chest deceleration and chest deflection of the occupant. For example, the vehicle deceleration can be lowered by securing sufficient vehicle deformation. The occupant chest deceleration can be lowered by limiting belt force. However, larger vehicle crush and occupant displacement are required for these countermeasures. Since a small car and micro mobility will become increasingly popular for environmental conservation, it is necessary to absorb the energy of the vehicle impact by shorter displacement. Therefore, to reduce thoracic injuries to older occupants, it would be beneficial to identify load paths from restraint systems to the thorax that provide higher stiffness in order to absorb higher kinetic energy of the occupant during a frontal collision. In the global thoracic response, the force-deflection response of the thorax differs under various loading conditions, such as single belt, double belt, hub [7-8], and the oblique thoracic response differs from the lateral thoracic response [9]. Stitzel et al. [10] and Cormier et al.

Y. Ito is engineer (tel: +81-80-9157-3066, e-mail: Yuichi_Ito@n.t.rd.honda.co.jp) and Y. Motozawa is chief engineer at Honda R&D Co., Ltd. Automobile R&D Center in Japan. F. Mori is engineer at PSG Co., Ltd. in Japan.

[11] defined the regional variation in the geometrical and material properties of the human rib cortical bone. In addition, Stitzel et al. [10] showed the changes in fracture patterns by incorporating variation of the rib material properties into a FE model. Ridella et al. [6] showed that the thoracic injury type changed from soft to bony tissue injury as age increased for frontal collisions. In order to identify load paths in the thoracic cage of older occupants, the authors attempted to understand the local response mechanism of the thoracic cage against various loadings such as a belt, airbag or other interior components.

The purpose of this study was to identify more general responses of the thorax to various loadings in order to address possible restraint systems with less aggressivity apart from constraint of the configuration of the conventional system. As the first stage, in order to understand the local response of the thorax, we developed distribution maps representing the local stiffness and tolerance of the rib cage against blunt loading using age-specific human occupant FE models. In addition, the effect of aging on the local response of the rib cage was investigated. In order to simulate the local rib cage response, the impact area on the rib cage was parametrically divided along the superior-inferior direction and the circumferential direction, and response analysis was conducted for 282 areas in total.

II. METHODS

Age-specific human occupant FE model

In this research, the age-specific human occupant FE model developed by Ito et al. [12-14], Dokko et al. [15-17] and Ito et al. [18] was used as shown in Figure 1. The age of the human occupant FE model was defined as 35 Y/O for the adult model and 75 Y/O for the elderly model by Ito et al. [12].

The adult and elderly occupant full body FE models were developed in order to simulate a car occupant's interaction with vehicle restraint systems. These FE models incorporated the lower limb, lumbar spine and thorax models previously developed by Ito et al. [12-14] and Dokko et al. [15-16]. The internal organ model was represented by seven simplified components modeled using solid elements. Figure 1 shows an oblique view of the adult occupant FE model, along with the model geometry of the rib cage of the adult and elderly. The rib cage of the elderly thoracic FE model used in this study was developed based on rib cage CT images representing the average anthropometry of an American Male (AM) 50th percentile elderly human subject at 75 Y/O. The rib cage CT images were extracted from the database of medical CT images at the University of Michigan Program for Injury Research and Education (UMPIRE). The translation vectors of rib angle associated with aging were determined based on the statistics. The adult thoracic FE model was developed by applying the vector to the elderly thoracic FE model. These rib cage models represented the change of the rib angle and spine curvature due to aging. In addition, the cortical bone thickness distribution of the rib and clavicle were established for the adult and the elderly based on Ito et al. [12] and applied to the FE models. The rib model was divided into 16 segments, 4 segments longitudinally and 4 segments circumferentially.

PAM-CRASH^{TM} was used as the FEM solver. The elastoplastic constitutive model was applied to the bones using the material type 143 for shell elements and 36 for solid elements. The linear viscoelastic constitutive model was applied to the solid elements representing the internal organs using the material type 5. The material parameters including the Young's modulus, yield stress, ultimate stress and strain of the femur, tibia, fibula, lumbar spine, clavicle, rib and sternum were determined from published human data. Bone stiffness parameters specified in the model were determined during the model validation process against published experiments of isolated bones by Ito et al. [12-14] and Dokko et al. [15-16]. Bone fracture was represented by using the element elimination option with a total strain criterion in PAM-CRASH^{TM}. Global response of the thoracic cage was validated against the pendulum impact tests by Kroell et al. [19-20] and the table-top thoracic belt loading tests by Kent et al. [7] in the published reports of Ito et al. [12-14]. The full body kinematics of the adult model was validated against frontal and side sled tests with Post Mortem Human Subjects (PMHSs) by Ito et al. [18] and Dokko et al. [17].

The age-dependent characteristics of the rib cage structure were accurately modeled with the age-specific human occupant FE models. Also, biofidelity validation was performed from the cortical bone specimen level to the component level against the present published biomechanical data. Therefore, the age-specific human occupant FE model was used to calculate the local response of the rib cage.

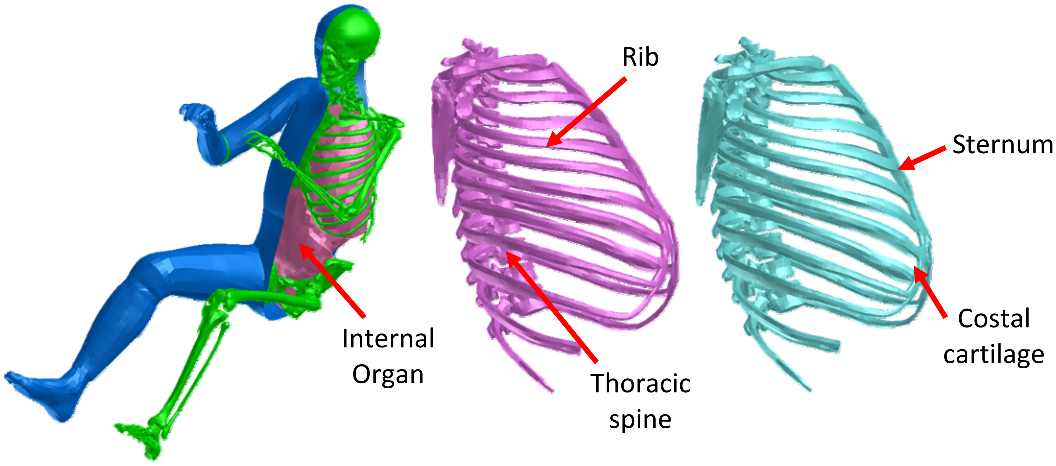

Fig. 1. Age-specific human occupant FE model (Ito et al. [18], Dokko et al. [17]). From left to right: full body model, adult (defined as 35 Y/O) rib cage model, elderly (defined as 75 Y/O) rib cage model.

Local thoracic response analysis

In order to develop a local stiffness and tolerance map of the thoracic cage, the thoracic response simulations against blunt loading were conducted by using the age-specific occupant FE models of 35 and 75 Y/O and a rigid spherical impactor model. The impactor was modeled using shell elements. The line perpendicular to the upper surface of the eighth vertebral body passing through its centrum was defined as the eighth thoracic vertebra axis, and the moving direction of the impactor was set perpendicular to the eighth thoracic vertebra axis. The degrees of freedom of the impactor other than the moving direction were constrained. As shown in Figure 2, the impact area on the thoracic cage was parametrically divided along the superior-inferior direction and the circumferential direction, and response analyses were conducted for 282 areas in total. Six levels of impact height were chosen from the umbilical level to the upper region at intervals of 50 mm along the superior-inferior direction. The circumferential direction was divided at intervals of 5 degrees from the right-hand side to the left-hand side by setting the eighth thoracic vertebra axis as the rotation center. In the present study, we analyzed the local thoracic response against pendulum loading. The validation of age-specific human occupant FE models used in the present study was done against the data of PMHS experiments conducted by Kroell et al. [19-20]. Based on the initial impact velocity, the response of the thorax was for a contact with a steering wheel without seat belt use. The initial velocities of the impactor were set at four different values of 2.5 m/s, 5.0 m/s, 10.0 m/s and 15.0 m/s In order to apply the same initial kinetic energy for each impact condition, the impactor mass was set at 80.0 kg, 20.0 kg, 5.0 kg and 3.2 kg, respectively.

In order to examine the thoracic response with different input conditions, the thoracic response simulation was conducted by using four different shapes of impactor as shown in Figure 3. The impactor type A is a spherical shape 50 mm in diameter; the impactor type B is a disk shape 150 mm in diameter; the impactor types C and D are elliptical in shape, measuring 150 mm by 50 mm. The impactor type C was horizontally positioned onto the thoracic cage, and impactor type D was perpendicularly positioned onto the thoracic cage. The initial velocity of the impactor was set at 5.0 m/s. The mass of the impactor was set at 20 kg. The input conditions of the simulation performed in this research are shown in table 1.

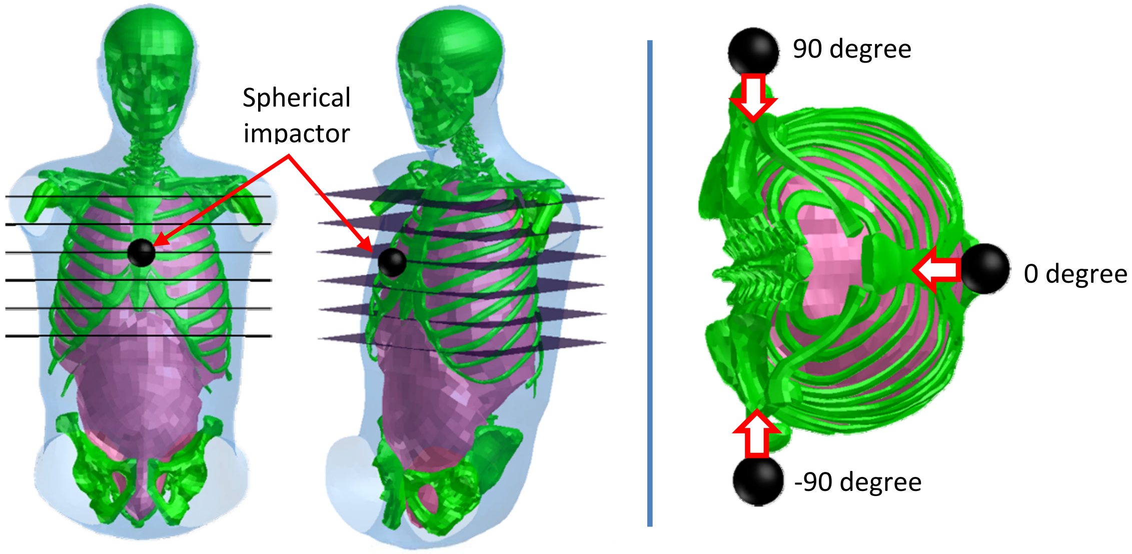

Fig. 2. Six levels of impact height were chosen from the umbilical level to the upper region at intervals of 50 mm along the superior-inferior direction. The circumferential direction is divided at intervals of 5 degrees from right-hand side (-90 degree) to left-hand side (90 degree).

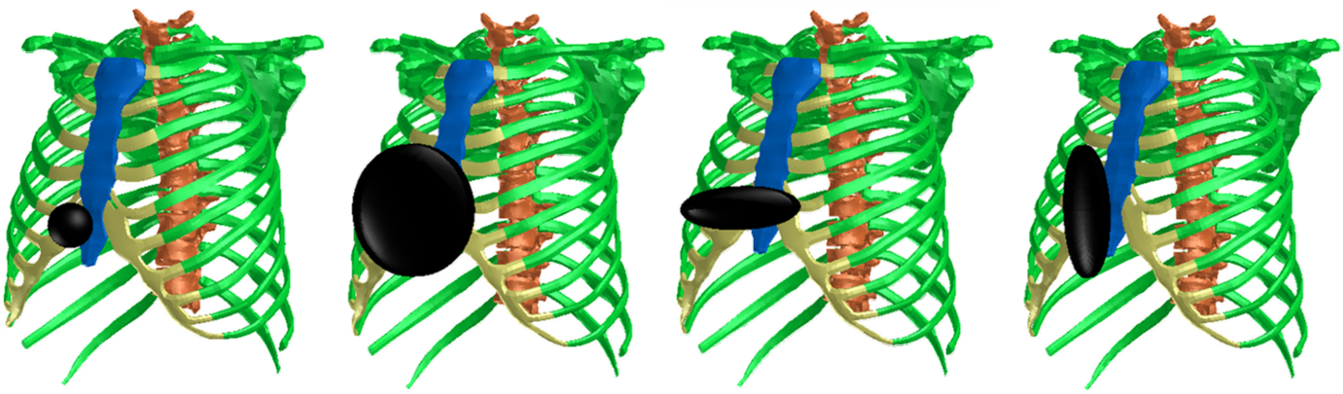

Fig. 3. Impactor type. From left to right: Type A (spherical ϕ50 mm), Type B (disk ϕ150 mm), Type C (ellipse 150×50 mm, horizontally), Type D (ellipse 50×150 mm, perpendicularly).

TABLE I
INPUT CONDITIONS

Impact Height (mm)	Impact Angle (degree)	Impact Initial Velocity (m/s)	Impactor Type
0 ～250 at intervals of 50 mm	-90 ～ 90 at intervals of 5 degrees	2.5	Type A (spherical ϕ50 mm)
		5.0	Type B (disk ϕ150 mm)
		10.0	Type C (ellipse 150×50 mm)
		15.0	Type D (ellipse 50×150 mm)

Calculated method of local thoracic stiffness and tolerance

Local stiffness of the thoracic cage was calculated by assuming a linear stiffness curve and using the energy absorbed up to 50 mm chest deflections. Local stiffness equation is

$$k = 2E/d^2 \quad (1)$$

where k is local stiffness of the thoracic cage (N/m), E is the deformation energy of the thoracic cage (Nm) and d is the chest deflection defined as the distance of the impactor moving direction between the eight thoracic spine center and an impactor center (m).

Local tolerance of the thoracic cage was defined from the value of the deflection where the element elimination was initially activated on the rib. If element elimination was not activated, when the chest deflection reached 80 mm, it was defined as "No Fracture".

III. RESULTS

Local stiffness and tolerance map of thoracic cage using spherical impactor

The local stiffness and tolerance were calculated based on the local thoracic response analysis using Equation 1. This paper shows the maps of the local stiffness and tolerance on the impactor initial velocity set at 5.0 m/s. The impact areas on the left side of the thoracic cage are only shown because the age-specific occupant FE model used in the study indicated almost symmetrical thoracic response. For each of the impact areas, the local stiffness of the thoracic cage is summarized in Figures 4 and 5. Figure 4 shows the local stiffness map of the adult occupant and Figure 5 shows the local stiffness map of the elderly occupant, respectively. In the impact area with 200 mm or higher and 50 degrees or larger in angle, the authors did not calculate stiffness because the impactor contacted the arm. Figures 6 and 7 show the local tolerance maps of both ages. The tolerance map of the impact height of 50 mm, 100 mm and 150 mm are shown in these graphs. The area where an element fracture did not activate when chest deflection reached 80 mm is shown as "No fracture". As shown in Figure 8, when the sternum is impacted from the frontal direction, the costal cartilage largely deforms like a hinge in advance of the rib deformation due to its lower stiffness, which maintains the shape of the rib with a smaller deformation. This is the mechanism that allows the chest deformation of 80 mm without rib element elimination as indicated in the results of the FE analysis.

The distribution of the local stiffness and tolerance map indicated identical tendency in both age groups, although their absolute values differed. In the impact height of 0 and 50 mm, the stiffness map indicated the smallest value around the impact angle of 0 degree and the largest around the impact angle of 60 degrees. In the impact height of 100 mm, 150 mm and 200 mm, the stiffness map indicated larger values in the impact angle of 0 degree and around the impact angle of 60 degrees, and indicated significantly smaller values around the impact angle of 20 degrees. In the impact height of 250 mm, the stiffness map indicated the largest value in the impact angle of 0 degree, indicating constant decrease with the increase of the impact angle. The largest stiffness in the thoracic cage was observed in the area of impact height of 250 mm and 0 degree in angle in both age groups. The maximum values of the stiffness were 51.8 kN/m for the adult and 43.6 kN/m for the elderly, respectively. The least stiffness was observed in the area of impact height of 0 mm and 0 degree in angle in both age groups. The minimum values of the stiffness were 7.2 kN/m for the adult and 5.6 kN/m for the elderly, respectively.

Around the impact angle of 0 degree larger values of the stiffness were observed than other areas. The smallest tolerance was observed around the impact area of 60 degrees. The values of the chest deflection at the time where element elimination was initially activated on the rib were 24.4 mm for the adult and 17.4 mm for the elderly.

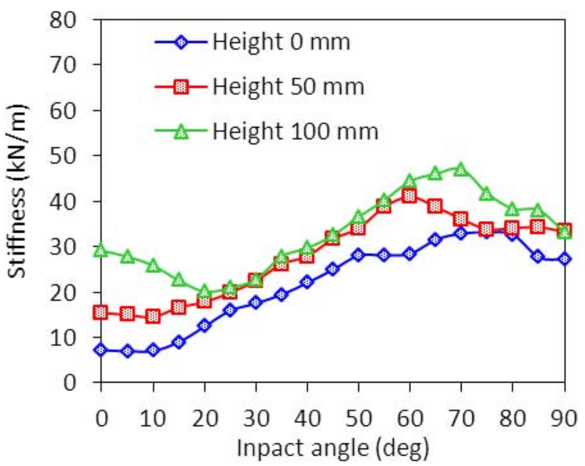

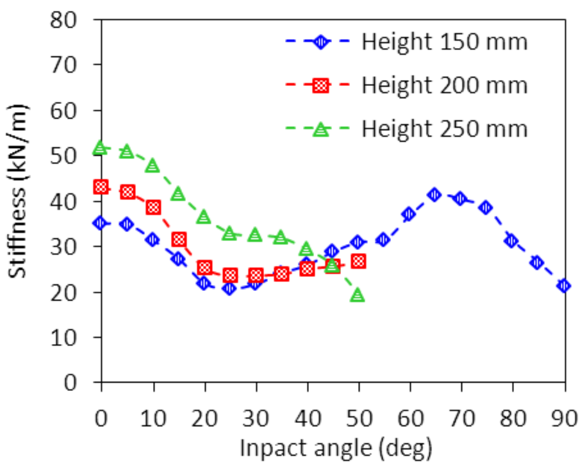

Fig. 4. Local stiffness maps of the adult thoracic cage from the impact angle of 0 to 90 degrees. Left side: impact height of 0, 50 and 100 mm. Right side: impact height of 150, 200 and 250 mm.

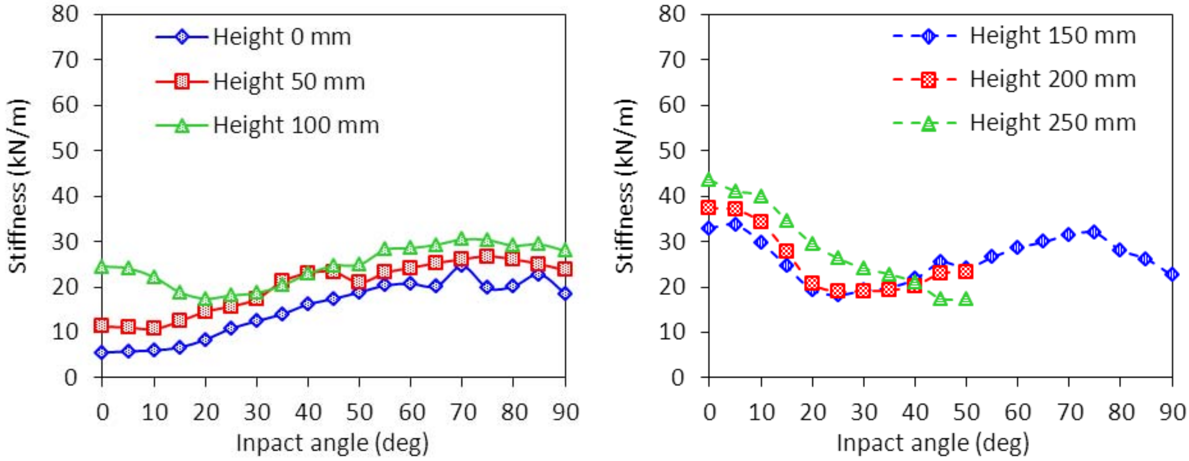

Fig. 5. Local stiffness maps of the elderly thoracic cage from the impact angle of 0 to 90 degrees. Left side: impact height of 0, 50 and 100 mm. Right side: impact height of 150, 200 and 250 mm.

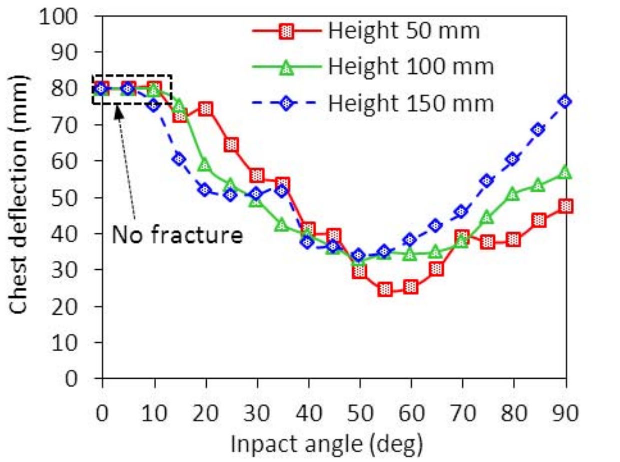

Fig. 6. Local tolerance maps of the adult thoracic cage from the impact angle of 0 to 90 degrees in the impact height of 50, 100 and 150 mm.

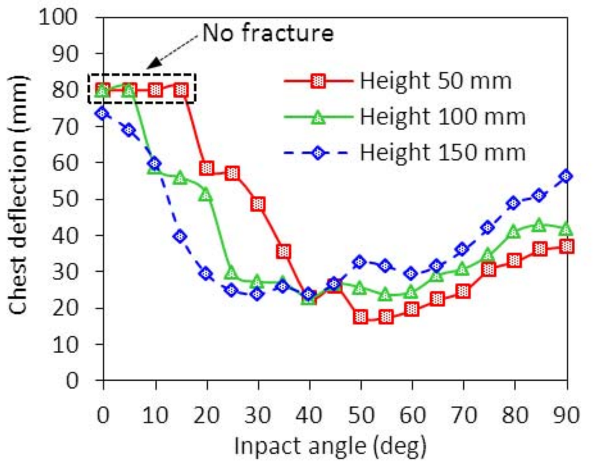

Fig. 7. Local tolerance maps of the elderly thoracic cage from the impact angle of 0 to 90 degrees in the impact height of 50, 100 and 150 mm.

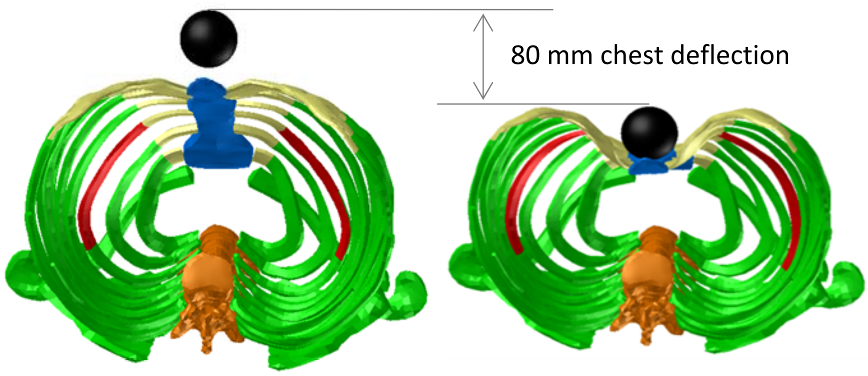

Fig. 8. Deformed shape of the thoracic cage in the bottom view under frontal impact loading from the age-specific human occupant model representing 75 Y/O in the impact from the spherical impactor simulations at the chest deflection of 80 mm (rib element elimination was not activated).

Response analysis accompanying rate dependence

Figures 9 and 10 show the local stiffness and tolerance of the elderly thoracic cage with different impactor velocities. Since the distribution of the local stiffness and tolerance maps indicated identical tendency in both age groups in the preceding paragraph, the representative results of the elderly are shown in this paragraph for the impact height of 150 mm and the impactor angle of 0 degree, 20 degrees and 60 degrees.

The local stiffness increased associated with the increment of the impactor velocity in any impact area as shown in Figure 9. At the impact velocity of 2.5 m/s, the values of local stiffness in the impact angle of 0 degree, 20 degrees and 60 degrees were at 23.4 kN/m, 14.4 kN/m and 22.8 kN/m, respectively. At the impact velocity of 15 m/s, the values of local stiffness in the impact angle of 0 degree, 20 degree and 60 degree areas were 78.1 kN/m, 46.1 kN/m and 59.0 kN/m, respectively. The values of local stiffness at impact velocity of 15 m/s were 3.3 times, 3.2 times and 2.6 times greater than those at the impact velocity of 2.5 m/s in impact angle of 0 degree, 20 degrees and 60 degrees, respectively. These results suggest a significant rate dependency of local stiffness in the frontal impact area.

Figure 10 indicates the tolerance of the thoracic cage, i.e. the value of the deflection where the element elimination was initially activated on the rib. Although the element elimination of rib was not activated until the impact velocity reached 5 m/s in the impact of 0 degree, the value of local tolerance indicated a decrease associated with the increase of the impact velocity as shown in Figure 9. At the impact velocity of 2.5 m/s, the values of local tolerance in the impact angle of 20 degrees and 60 degrees were 40.2 mm and 35.8 mm, respectively. At the impact velocity of 15 m/s, the value of local tolerance in the impact angle of 0 degree, 20 degree and 60 degree were 63.6 mm, 20.9 mm and 25.2 mm, respectively. At the impact velocity of 2.5 m/s, the values of local tolerance were 1.9 times and 1.4 times greater than those at the impact velocity of 15 m/s in the impact angle of 20 degrees and 60 degrees, respectively. These suggest significant rate dependency of local tolerance in oblique impacts.

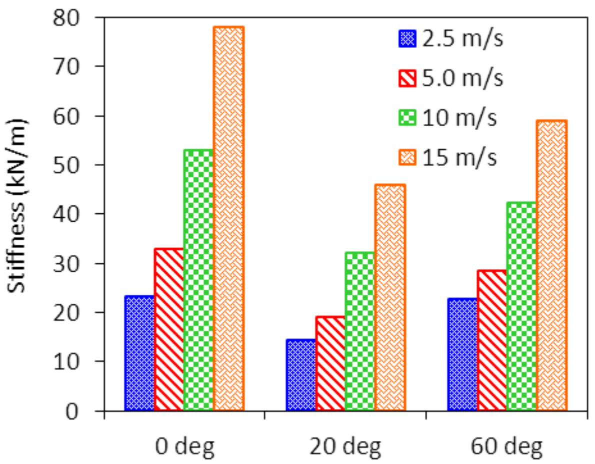

Fig. 9. Local stiffness of the elderly thoracic cage with different impact velocities in impact angle of 0, 20 and 60 degrees at impact height of 150 mm.

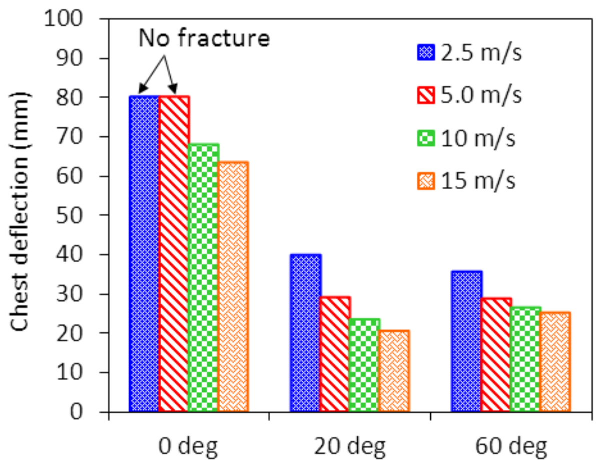

Fig. 10. Local tolerance of the elderly thoracic cage with different impact velocities in impact angle of 0, 20 and 60 degrees at impact height of 150 mm.

Response analysis accompanying input conditions (impactor shape)

Figure 11 shows the local stiffness with different impactor shapes. The simulation results of the elderly for the impactor height of 100 mm and the impactor angle of 0 degree, 20 degrees and 60 degrees are described below. Similarly, Figure 12 shows the local tolerance with different impactor shapes.

The disk impactor with the largest surface area indicated the largest stiffness in any impact area as shown in Figure 11. For the spherical impactor, the values of local stiffness in the impact angle of 0 degree, 20 degrees and 60 degrees were 24.5 kN/m, 17.4 kN/m and 28.6 kN/m, respectively. For the disk impactor, the values of local stiffness in the impact angle of 0 degree, 20 degrees and 60 degrees were 42.5 kN/m, 37.6 kN/m and 60.5 kN/m, respectively. The disk impactor had local stiffness 1.7 times, 2.2 times and 2.1 times greater than the spherical impactor, respectively. Local tolerance of the disk impactor was less than the spherical impactor in any area.

The ellipse impactor had larger local stiffness than the spherical impactor, but the ellipse impactor indicated the difference of thoracic response with impactor direction. Comparing the direction of the impactor horizontally and perpendicularly as placed onto the thoracic cage, the impactor placed horizontally had larger stiffness and less tolerance than the impactor placed perpendicularly in the impact angle of 0 degree and 20 degrees. The impactor placed horizontally had less stiffness and larger tolerance than the impactor placed perpendicularly in the impact angle of 60 degrees.

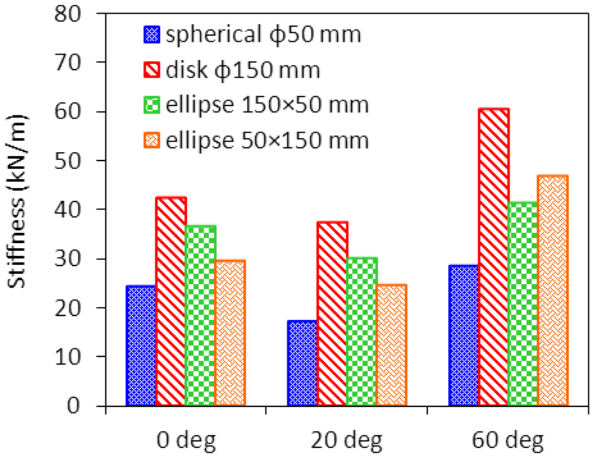

Fig. 11. Local stiffness of elderly thoracic cage with different impactor shapes in impact angle of 0, 20 and 60 degrees at impact height of 100 mm.

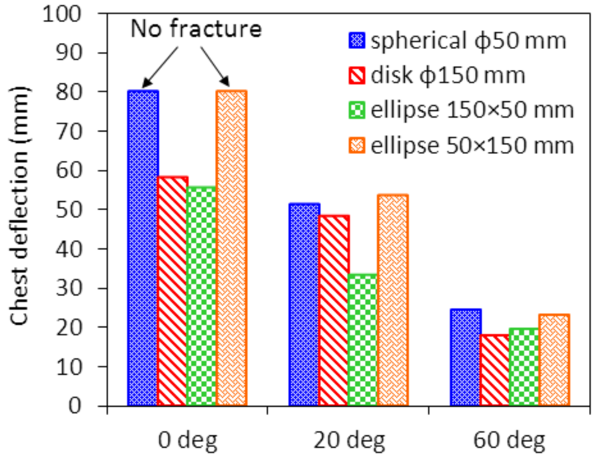

Fig. 12. Local tolerance of elderly thoracic cage with different impactor shapes in impact angle of 0, 20 and 60 degrees at impact height of 100 mm.

IV. DISCUSSION

Distribution of stiffness and tolerance of thoracic cage

As shown in Figures 4 through 7, the comparison of the response between the adult occupant and the elderly occupant clearly presented the quantitative difference in the local stiffness and tolerance of the thoracic cage associated with aging. The distribution in the local stiffness and tolerance map indicated an identical tendency in both age groups. It was found that the local stiffness and tolerance of the elderly thoracic ribcage are significantly less than that of the younger adult thoracic rib cage which suggests that the elderly have a higher possibility of bony injuries compared to younger adults in any area.

The distribution of the local stiffness indicated identical tendency in both age groups. The local stiffness increase was found to be associated with the increment of the impact height. Also the local stiffness was higher than the other area at around 0 degree (frontal area) and 60 degrees (lateral area) of the impact angle, and lower at around 20 degrees (oblique area) of the impact angle. These results indicated the heterogeneity of the global thoracic response as a consequence of the complexity of the thoracic cage geometry. In a frontal impact, the majority of the load is normally transmitted through the sternum. The high stiffness of the frontal area would be due to the load distribution to the internal organs and the ribs via the sternum. When load is applied to either the oblique area or lateral area, the load is mainly transmitted through the costal cartilage or the ribs. It is suggested that the local stiffness of these areas depends on the bending stiffness of the costal cartilage and the ribs. The local thoracic stiffness of the lateral area is larger than the oblique area, because the rib is stiffer than the costal cartilage [12]. The inhomogeneous local stiffness of the thoracic cage suggests that the difference of the stiffness between the areas would contribute to the difference in the global chest deflection.

The distribution of the local tolerance indicated identical tendency in both age groups. The local tolerance was found to be larger in the frontal area and less in the lateral area. Figure 13 shows the deformed shape of the thoracic cage in the bottom view in spherical impactor loading at the chest deflection of 50 mm. In the case of the frontal area, the ribs were loaded through the sternum and the costal cartilage. Due to the large deformation of the costal cartilage, it is considered that the deformation of the ribs is less than those in other areas. In the case of the lateral area, the impactor loading was concentrated on the ribs, so the ribs deformed locally as shown in Figure 13. The comparison of the maps of the local stiffness and tolerance for the adult and the elderly explains why an elderly occupant is more likely to sustain injury to the thorax compared with an adult occupant in the case of a frontal collision.

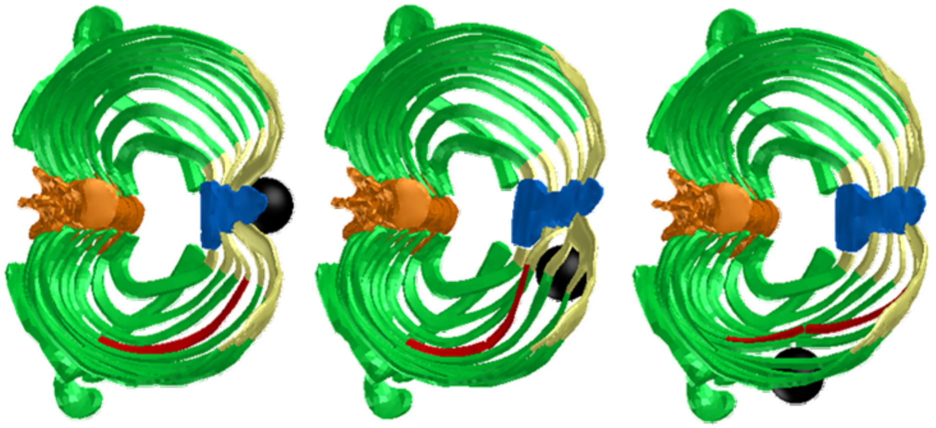

Fig. 13. Deformed shape of the thoracic cage in the bottom view under different loading angles from the age-specific human occupant model representing 75 Y/O in the impact from the spherical impactor simulations. From left to right: impactor angle is 0 (frontal area), 20 (oblique area) and 60 degrees (lateral area).

Examination of influence of impactor velocity

The local stiffness increase was found to be associated with the increment of the impactor velocity in any impact areas. It is considered that the rate dependency of the thoracic cage comes from the viscosity of the soft tissues such as the flesh and the internal organs. The rate dependency was more evident in the frontal area than in the oblique or lateral area. This would be due to the larger distribution of the load to the highly viscoelastic internal organs via the sternum than the other areas.

The local tolerance decrease was found to be associated with the increment of the impactor velocity in any area. Figure 14 shows the deformed shape of the thoracic cage in the bottom view at different loading velocities at the chest deflection of 50 mm in an oblique impact area. Even if the global chest deflection was independent of the impact velocity, the local rib deformation was larger at higher impact velocities.

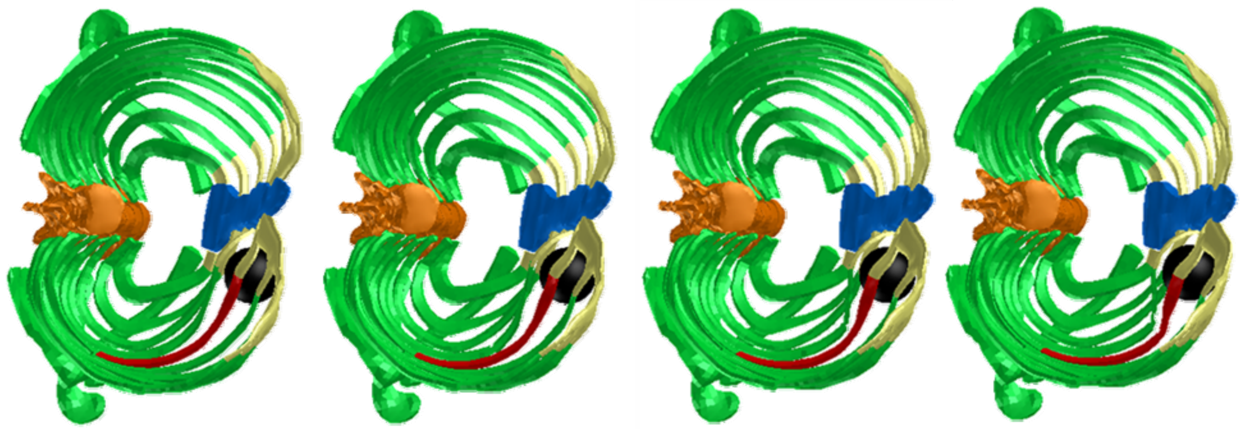

Fig. 14. Deformed shape of the thoracic cage in the bottom view at different loading velocities from the age-specific human occupant model representing 75 Y/O in the impact from the spherical impactor at the chest deflection of 50 mm in an oblique impact area. From left to right: impactor initial velocity set at 2.5 m/s, 5.0 m/s, 10 m/s, 15 m/s.

Examination of influence of input conditions (impactor shape)

The local stiffness obtained from the impact from the disk impactor with the diameter of 150 mm was larger than that from the spherical impactor with the diameter of 50 mm in each of the impact areas. This suggests that the load distribution effectively increases the global thoracic stiffness. However, the local tolerance from the disk impactor was less than that from the spherical impactor. Figure 15 shows the deformed shape of the thoracic cage in the bottom view in an impact from the impactors with different shapes at the chest deflection of 60 mm in the frontal impact area. In the spherical impactor, the deformation of the costal cartilage is larger than other impactors due to the localized loading to the sternum. In contrast, in the disk impactor, the deformation of the ribs is large, due to the direct loading to the ribs. Therefore, the chest deformation at the time of the rib element elimination was smaller with the disk impactor than the spherical impactor. Figure 15 shows the deformed shape of the thoracic cage in an impact from different impactors at the chest deflection of 50 mm in the frontal impact area. Although the impact load was distributed to the ribs for any of the impactors, the amount of the overlap between the impactors and the ribs differed due to the difference in the shape of the impactors. It is suggested that the stiffness and tolerance of the thoracic cage would change due to the change in the load path associated with impactor shape under the realistic loading velocity from the pendulum loading.

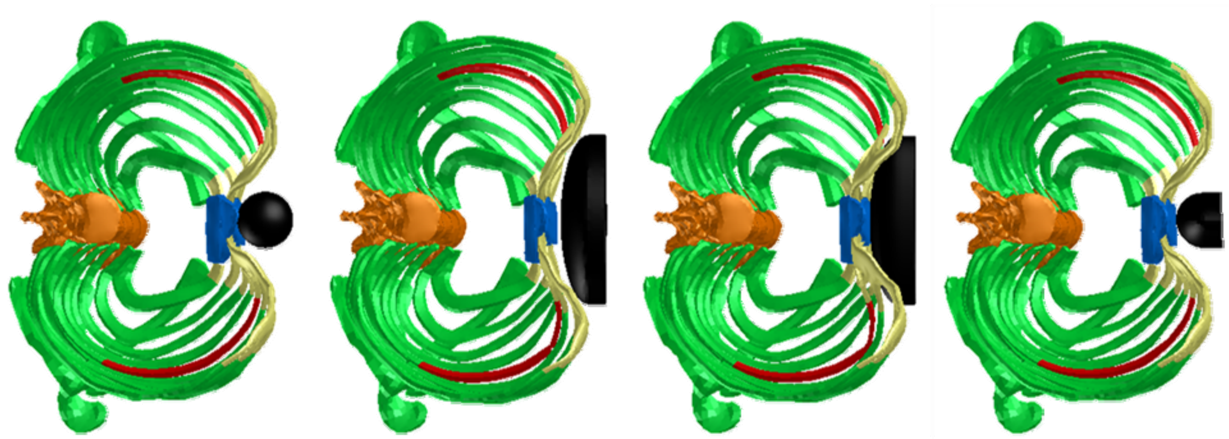

Fig. 15. Deformed shape of the thoracic cage in the bottom view under different loading conditions from the age-specific human occupant model representing 75 Y/O with impactor initial velocity set at 5.0 m/s at the chest deflection of 60 mm in the frontal impact area. From left to right: impactor type is spherical (ϕ50 mm), disk (ϕ150 mm), ellipse (150×50 mm), ellipse (50×150 mm).

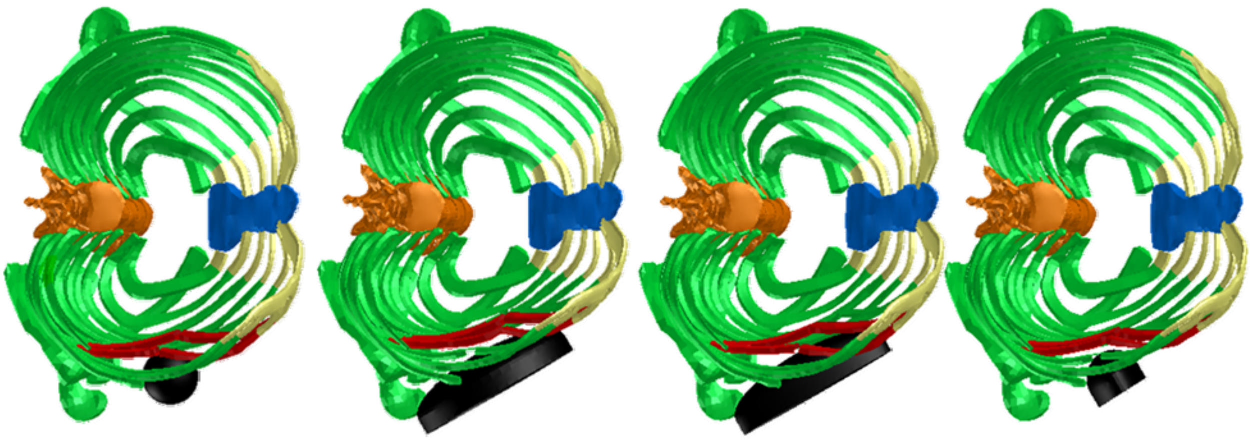

Fig. 15. Deformed shape of the thoracic cage in the bottom view under different loading conditions from the age-specific human occupant model representing 75 Y/O with the impactor initial velocity set at 5.0 m/s at the chest deflection of 50 mm in the lateral impact area. From left to right: impactor type is spherical (ϕ50 mm), disk (ϕ150 mm), ellipse (150×50 mm), ellipse (50×150 mm).

V. CONCLUSIONS

The thoracic response simulations were conducted using the age-specific human occupant FE models under pendulum loading with various impact areas, impact velocities and impactor shapes. In order to develop the maps of the local stiffness and tolerance of the thoracic cage, the local response of the thoracic cage was calculated for 282 areas in total. In addition, the effects of the rate dependency and the loading conditions were also investigated. The local stiffness and tolerance maps were quantitatively calculated for different ages represented by the human models. The difference of the local thoracic response due to aging was shown. It was also found that the local stiffness and tolerance of the elderly thoracic cage were less than those of the adult. This explains the fact that the elderly occupants are more likely to sustain injury to the thorax compared with younger adult occupants in frontal collisions. However, the distribution of the local stiffness and tolerance maps indicated identical tendency in both age groups. It was shown that the local response varied regionally under pendulum loading. Larger local stiffness was indicated in the frontal and lateral areas, while less local stiffness was indicated in oblique areas. It was found that the local stiffness and tolerance of the thoracic cage is not homogeneous in any age group, which suggested that the difference in the input area may cause the difference in the global chest deflection. Also, it was shown that the local response of the thoracic cage changed with the input velocity and input condition.

VI. REFERENCES

[1] Statistics Bureau Director-General for Policy Planning & Statistical Research and Training Institute, "Growth of Population" http://www.stat.go.jp/english/data/nenkan/1431-02.htm

[2] U.S. Department of Health and Human Services, *A Profile of Older Americans*, 2011

[3] Institute of Traffic Accident Research and Data Analysis, *Traffic Accident Statics*, 2000-2011 (in Japanese).

[4] Institute of Traffic Accident Research and Data Analysis, *ITARDA Information*, 2003, No.41.

[5] Institute of Traffic Accident Research and Data Analysis, *ITARDA Information*, 2007, No.71.

[6] Ridella SA, Rupp JD, Poland K, Age-related differences in AIS 3+ crash injury risk, types, causation and mechanisms, *Proceedings of IRCOBI Conference,* 2012, Ireland, Dublin, pp. 43-60.

[7] Kent R, Lessley D, Sherwood C, Thoracic response to dynamic, non-impact loading from a hub, distributed belt, diagonal belt, and double diagonal belts, *Stapp Car Crash Journal, 2004, 48:495-519.*

[8] Kent R, Murakami D, Kobayashi S, Frontal thoracic response to dynamic loading: the role of superficial tissues, viscera, and the rib cage, *Proceedings of IRCOBI Conference,* 2005, Praha, Czech Republic, pp. 355-365.

[9] Shaw JM, Oblique and lateral impact response of the PMHS thorax, S*tapp Car Crash Journal,* 2006, 50:147-167.

[10] Stitzel JD, Cormier JM, Barretta JT, Kennedy EA, Smith EP, Rath AL, Duma SM, Matsuoka F, Defining regional variation in the material properties of human rib cortical bone and its effect on fracture prediction, *Stapp Car Crash Journal,* 2003, 47:243-265.

[11] Cormier JM, Stitzel JD, Duma SM, Matsuoka F, Regional variation in the structural response and geometrical properties of human ribs, *Annu Proc Assoc Adv Automot Med,* 2005, 49:153-170.

[12] Ito O, Dokko Y, Ohashi K, Development of adult and elderly FE thorax skeletal models, *SAE World Congress*, 2009, Detroit, USA, 2009-01-0381.

[13] Ito O, Dokko Y, Ohashi K, Development of thorax skeletal FE models for adult and the elderly, *Transactions of JSAE*, 2009, 40(6):1457-1462.

[14] Ito O, Ito Y, Dokko Y, Mori F, Ohhashi K, Development of adult and elderly FE thorax models (Second Report), *Transactions of JSAE,* 2011, 42(3):703-708.

[15] Dokko Y, Ito O, Ohashi K, Development of human lower limb and pelvis FE models for adult and the elderly, *SAE World Congress*, 2009, Detroit, USA, 2009-01-0396.

[16] Dokko Y, Kanayama Y, Ito O, Ohashi K, Development of human lumbar spine FE models for adult and the elderly, *SAE World Congress*, 2009, Detroit, USA, 2009-01-0382.

[17] Dokko Y, Yanaoka T, Ohashi, K, Validation of age-specific human FE models for lateral impact, *SAE World Congress*, 2013, Detroit, USA, 2013-01-1242.

[18] Ito Y, Dokko Y, Motozawa Y, Mori F, Ohashi K, Kinematics validation of age-specific restrained 50th percentile occupant FE model in frontal impact, *SAE World Congress*, 2012, Detroit, USA, 2012-01-565.

[19] Kroell C, Schneider D, Nahum A, Impact tolerance and response of the human thorax, SAE Technical Paper #710851, 1971.

[20] Kroell C, Schneider D, Nahum A, Impact tolerance and response of the human thorax II, SAE Technical Paper #741187, 1974.